Kenfen Li, Yanping Zhang, Yunfeng Wang, Xin Guo, Xianhui Dai and Li Song*

The lncRNA prostate androgen-regulated transcript 1 (PART-1) promotes non-small cell lung cancer progression by regulating the miR-204-3p/IGFBP-2 pathway

https://doi.org/10.1515/labmed-2022-0082
Received July 30, 2022; accepted January 11, 2023;
published online February 2, 2023

Abstract

Objectives: Lung cancer is a common malignant tumour of the lung and the leading cause of cancer mortality worldwide. Non-small cell lung cancer (NSCLC) accounts for 80–85% of lung cancers, and 40% of NSCLCs have spread beyond the lungs by the time they are diagnosed. The long noncoding RNA (lncRNA) prostate androgen-regulated transcript 1 (PART-1) has been reported to promote the development of several cancers.
Methods: In the current study, we investigated the role of PART-1 in the proliferation, invasion, and migration of NSCLC.
Results: The expression levels of the PART-1 gene were higher in NSCLC cell lines, including A549, H1229, H1650, H1975, and PC9, than in human bronchial epithelia (HBE) cell lines. Knocking down PART-1 inhibited the proliferation, invasion, and migration of A549 cells and decreased tumour proliferation in nude mice. We confirmed that PART-1 targeted miR-204-3p directly and that miR-204-3p targeted insulin-like growth factor binding protein 2 (IGFBP-2) directly. Furthermore, we discovered that PART-1 impacts NSCLC progression by regulating the miR-204-3p-targeted IGFBP-2 pathway.
Conclusions: The lncRNA PART-1 might be a target for treating NSCLC and an early marker in the diagnosis of early lung cancer.

Keywords: insulin-like growth factor binding protein 2; long noncoding RNA; miR-204-3p; prostate androgen-regulated transcript 1.

***Corresponding author: Li Song**, Department of Respiratory Medicine, Shanghai Eighth People's Hospital, Shanghai, Shanghai, P.R. China, E-mail: 147150379@qq.com
Kenfen Li, Yanping Zhang, Yunfeng Wang, Xin Guo and Xianhui Dai, Department of Respiratory and Critical Care Medicine, People's Hospital of Chengyang District, Qingdao, P.R. China

Introduction

Lung cancer is a common malignant tumour of the lung and the leading cause of cancer-related death [1]. Most lung cancers are diagnosed at an advanced stage because of an absence of clinical symptoms or due to a lack of effective screening programs [1]. The incidence of lung cancer has been on the rise globally, and lung cancer is the leading cause of cancer mortality worldwide [2]. Although the mechanistic understanding, treatment options, and outcomes for lung cancer are improving, 5-year survival continues to be low [3]. Lung cancer can be divided into small cell lung cancer (SCLC) and non-small cell lung cancer (NSCLC) according to the histopathological characteristics of the lesion [4]. NSCLC accounts for 80–85% of lung cancers, and each type of NSCLC comprises different kinds of cancer cells, which grow and spread in different ways [5]. Although a large number of different markers have been proposed to predict the risk of NSCLC progression, few of them are used in clinical practice [5].

Long noncoding RNAs (lncRNAs) are defined as transcripts greater than 200 nucleotides that are transcribed by RNA polymerase II but not translated into proteins [6]. Although the function of lncRNAs is still debated, a growing number of lncRNAs are well documented to have important cellular functions [7, 8]. LncRNAs play roles in gene regulation by acting as activators or decoys for transcription factors, recruiters of chromatin-modifying complexes, miRNA sponges, and scaffolds of molecular complexes [7]. LncRNAs can regulate mRNAs through shared miRNAs and play critical roles in the development of tumours by acting as competing endogenous RNAs (ceRNAs) [9], and the dysregulation of their expression is observed in numerous diseases [10].

During carcinogenesis, the alteration of lncRNA expression may have oncogenic effects (for example, NCK1-AS1 promotes cancer cell proliferation and increases cell stemness in urinary bladder cancer [11]) or tumour suppressive effects (for example, TSLNC8 inhibits the proliferation of breast cancer cells [12]). To date, several lncRNAs have been reported

to possess promising prognostic or diagnostic value for NSCLC [8, 13–15]. Nevertheless, there is an urgent need to identify novel biomarkers to support the development of an effective, convenient, and economical method for the early diagnosis, early detection, and early treatment of lung cancer in clinical practice [8].

Prostate androgen-regulated transcript 1 (PART-1) is one lncRNA of potential value. PART-1 was discovered in 2000 and is expressed in prostate tissue and regularizes androgens in prostate cancer cell lines [16]. PART-1 promoted prostate cancer cell proliferation and inhibited cell apoptosis and was associated with worse outcomes and poorer survival among prostate cancer patients [24]. Moreover, PART-1 serves as an oncogenic lncRNA by sponging miR-590-3p to upregulate HMGB2 expression in hepatocellular carcinoma [17]. In addition, PART-1 was associated with worse outcomes in colorectal cancer via activation of the Wnt/beta-catenin pathway and sponging miR-150-5p/miR-520 h [18]. Accordingly, we hypothesized that PART-1 may have a crucial role in NSCLC development.

In the current study, the expression and roles of PART-1 were investigated in NSCLC, and the potential underlying regulatory mechanism was revealed. We determined that PART-1 served as a competing endogenous RNA by sponging miR-204-3p and regulated the miR-204-3p/IGFBP-2 pathway to promote NSCLC progression.

Materials and methods

Cell lines

Human NSCLC cell lines, including A549, H1299, H1650, H1975, and PC9, and a human bronchial epithelial (HBE) cell line were purchased from the National Collection of Authenticated Cell Cultures. The cell lines were maintained in Dulbecco's modified Eagle's medium (DMEM; Invitrogen, Carlsbad, CA, USA) supplemented with 10% foetal bovine serum (FBS; Sigma–Aldrich, St. Louis, MO, USA), 100 U/mL penicillin and 100 mg/mL streptomycin (Invitrogen, Carlsbad, CA, USA) at 37 °C with 5% CO_2.

Quantitative reverse transcriptase PCR analysis

The mRNA expression levels were determined by quantitative RT–PCR in a Light-Cycler® 96 System Real-Time PCR System (Roche, USA) using Taq Pro Universal SYBR qPCR Master Mix (Q712–02, Vazyme, China). All of the primers were synthesized at Sangon Biotech (Shanghai) Co., Ltd. The primer sequences were as follows: PART-1, forward: 5′- AAG GCC GTG TCA GAA CTC AA-3′; and reverse: 5′- GTT TTC CAT CTCA GCC TGG A-3′ [19]; miR-204-3p, forward: 5′-ACA CTC CAG CTG GGG CTG GGA AGG CAA AGG G-3′ and reverse: 5′-CTC AAC TGG TGT CGT GGA-3′ [20]; IGFBP-2, forward: 5′-TGC ACA TCC CCA ACT GTG AC-3′ and reverse 5′-TGT AGA AGA GAT GAC ACT CGG G-3′ [21]; and GAPDH, forward: 5′-TGA CGC TGG GGC TGG CAT TG-3′ and reverse: 5′-GCT CTT GCT GGG GCT GGT GG-3′ [20]. GAPDH was used as an internal control for the quantification of gene targets. The PCR program consisted of denaturation at 95 °C for 30 s followed by 40 cycles of denaturation at 95 °C for 15 s and annealing at 60 °C for 30 s. The PCR products were subjected to melting curve analysis to test primer specificity. Three independent biological replicates and three technical replicates were analysed for each treatment. The relative expression levels of the mRNAs were analysed using the $2^{-(\Delta\Delta Ct)}$ method.

Transfection *in vitro*

Transfection experiments were conducted *in vitro*, and cells were seeded into 12-well culture plates (1×10^5 cells per well). When cells reached 80–90% confluence, the DNAs, including the miR-204-3p mimic, shRNA-PART1, miR204-3 inhibitor, and the other plasmids used in this study (as 4 μg plasmid and 246 μL serum-free medium (SFM)), were transfected into the cells with Lipofectamine 2,000 (Invitrogen, Shanghai, China) according to the manufacturer's instructions. Following incubation for 24 h, the cells were lysed for further use. The shRNA-PART1, miR204-3 inhibitor, pmiR-GLO vector, and miR-204-3p mimic were purchased from Shanghai GenePharma Co., Ltd, Shanghai, China.

Cell viability assay

The viability of A549 cells was measured using a Cell Counting Kit-8 assay (CCK-8) kit (AbMole BioScience, Shanghai, China). Cells (1×10^3 cells/well) were seeded in 96-well plates, grown for 24 h, 48 h, 72 h, or 96 h, and then 10 μL of CCK-8 solution was added to the wells and incubated for 4 h. The absorbance was measured at 450 nm using a microplate reader (Model 680 microplate reader, Bio-Rad Laboratories). Triplicate wells were prepared for each sample, and the experiments were repeated three times.

Cell colony formation

The transfected A549 cells were seeded into a 6-well culture plate (1,000 cells per well), covered with trypsin–EDTA solution and incubated at 37 °C until they became detached. Cells were cultured with RPMI-1640 medium for 3 weeks, at which time colonies were formed. Then, the medium was discarded, and the cells were washed twice with phosphate-buffered saline (PBS). Cells were fixed with 4% paraformaldehyde for 30 min at room temperature (RT), and subsequently, the colonies were stained with 1% crystal violet for 5 min at room temperature. The cells were washed with water until excess dye was removed, and the number of colonies was counted. Four cell wells were prepared for each sample, and the experiment was repeated four times at different times.

Transwell migration assay

Transfected A459 cell culture (100 μL) was plated onto the upper chamber coated with 50 μL of Matrigel matrix and incubated for 10 min at 37 °C and 5% CO_2 to allow the cells to settle. Then, 600 μL of DMEM supplemented with 10% foetal bovine serum (FBS) was added to the lower chamber. After incubating for 48 h, cells that invaded through the

membrane were fixed with 4% paraformaldehyde and then stained with 1% crystal violet for 15 min. The invading cells were photographed under a microscope at 200 × magnification (Olympus). Five fields of vision were investigated for each treatment, and the average number of invading cells was counted. Four cell wells were prepared for each sample, and the experiment was performed in triplicate.

Wound healing assay

A549 cells from each group were plated into a 6-well plate at a density of 5×10^5 cells per well. The cell monolayer was scratched using a sterile pipette tip when the cells reached 80% confluence, and then the cells were washed with PBS. Serum-free medium was added to the plates, and then the plates were kept in an incubator at 37 °C for 24 h. Wound closure was monitored and imaged at 0 and 24 h under a microscope (Olympus). The migration rate was calculated as (wound width at 0 h–wound width at 24 h)/wound width at 0 h × 100%. This experiment was conducted in triplicate for each group.

Xenograft tumour experiment

A total of 10 BALB/c nude mice were randomly and blindly divided into two groups (n=5 per group). A549 cells transfected stably with sh-PART1 or sh-NC were harvested. The cells (1×10^7 cells per treatment) were inoculated subcutaneously into the axilla of nude mice to generate the A549 tumour mouse model. The tumour volumes were monitored every 3 days from the sixth day after inoculation and calculated using the following formula: volume = 0.5 × length × width^2. After three weeks of treatment, the mice were euthanized, and the tumours were excised and weighed.

Luciferase reporter assay

The wild-type (WT) or mutant (MT) 3′-UTR of PART-1 containing the putative binding sites of miR-204-3p was inserted into the pmiR-GLO vector, and the reporter plasmids were named pMIRGLO-PART1-3′UTR and pMIRGLO-PART1-3′UTR-mutant, respectively. A549 cells were cotransfected transiently with the WT or MT 3′-UTR reporter plasmids of PART-1 and the miR-204-3p mimic in the presence of a luciferase reporter vector. In addition, the wild-type (WT) or mutant (MT) 3′-UTR of IGFBP containing the putative binding sites of miR-204-3p was also inserted into the pmiR-GLO vector. A549 cells were cotransfected transiently with WT or MT 3′-UTR reporter plasmids of IGFBP and miR-204-3p mimic in the presence of a luciferase reporter vector. The cells were harvested after 48 h of transfection, and the dual-luciferase reporter system (Promega, Madison, WI, USA) was used to determine the promoter activity. The experiment was repeated three times.

Western blot

Protein was extracted from A549 cells with RAPI lysis buffer (Solarbio, Beijing, China). The protein concentration was evaluated using a bicinchoninic acid (BCA) assay kit (Beyotime, Shanghai, China). A total of 15 μg of protein was loaded in each well and separated by 15% SDS–PAGE, and then the proteins were transferred onto a polyvinylidene difluoride (PVDF) membrane (Millipore, Braunschweig, Germany). The membrane was blocked with 5% nonfat milk for 1 h and incubated with primary antibodies for 2 h, followed by incubation of the membrane with goat anti-rabbit IgG secondary antibody (1:3,000, Bio-Rad, CA, USA). The membrane was imaged in an ECL imaging system, and the images were quantified to determine the intensities of the protein bands using ImageJ software (https://imagej.nih.gov/ij/). GAPDH was used as the loading control in this experiment.

Statistical analysis

SPSS 19.0 software (SPSS Inc., Chicago, IL, USA) was used to analyse the data. The results are expressed as the mean ± standard deviation from three or four independent experiments. To determine how the treatment levels differed from one another, unpaired Student's t test or one-way ANOVA was used, followed by Dunnett's post hoc test. The data were considered statistically significant when $p<0.05$.

Results

PART-1 was upregulated in the NSCLC cell lines

We detected the expression level of prostate androgen-regulated transcript 1 (*PART-1*) in the human bronchial epithelial (HBE) cell line and the human non-small cell lung cancer (NSCLC) cell lines, including A549, H1229, H1650, H1975, and PC9, by quantitative RT–PCR. The expression level of the PART-1 gene was 3.15, 2.78, 2.24, 1.9, and 1.71 times higher in the various NSCLC cell lines than in HBE cells ($p<0.05$) (Figure 1).

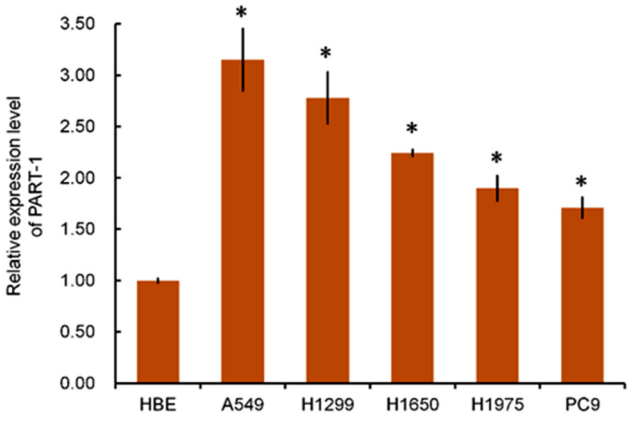

Figure 1: The expression of PART-1 in the HBE cell line and NSCLC cell lines, including A549, H1229, H1650, H1975, and PC9, as assayed by quantitative RT–PCR. The expression level of the PART-1 gene increased significantly in NSCLC cell lines. *Indicates $p<0.05$.

Knocking down PART-1 inhibited the proliferation, invasion, and migration of A549 cells

We knocked down PART-1 by lentiviral shRNA and generated two types of A549 cells: cells with silenced PART-1 (sh-PART1 group) and cells transfected with a noncoding shRNA (sh-NC group). The expression level of PART-1 in sh-PART1 cells was 0.557 times that in sh-NC cells by RT–PCR (Figure 2A).

The proliferation of transfected A549 cells was measured by the CCK-8 kit. The transfected cells were selected by puromycin and then monitored continuously for 96 h. The OD values of sh-PART1 cells and sh-NC cells increased with time; however, the value of sh-NC cells increased faster than that of sh-PART1 cells, and the OD values of sh-PART1 cells were significantly lower than those of sh-NC cells after 96 h of incubation (Figure 2B). The results demonstrated that proliferation of A549 cells was inhibited by the downregulation of PART-1. The average

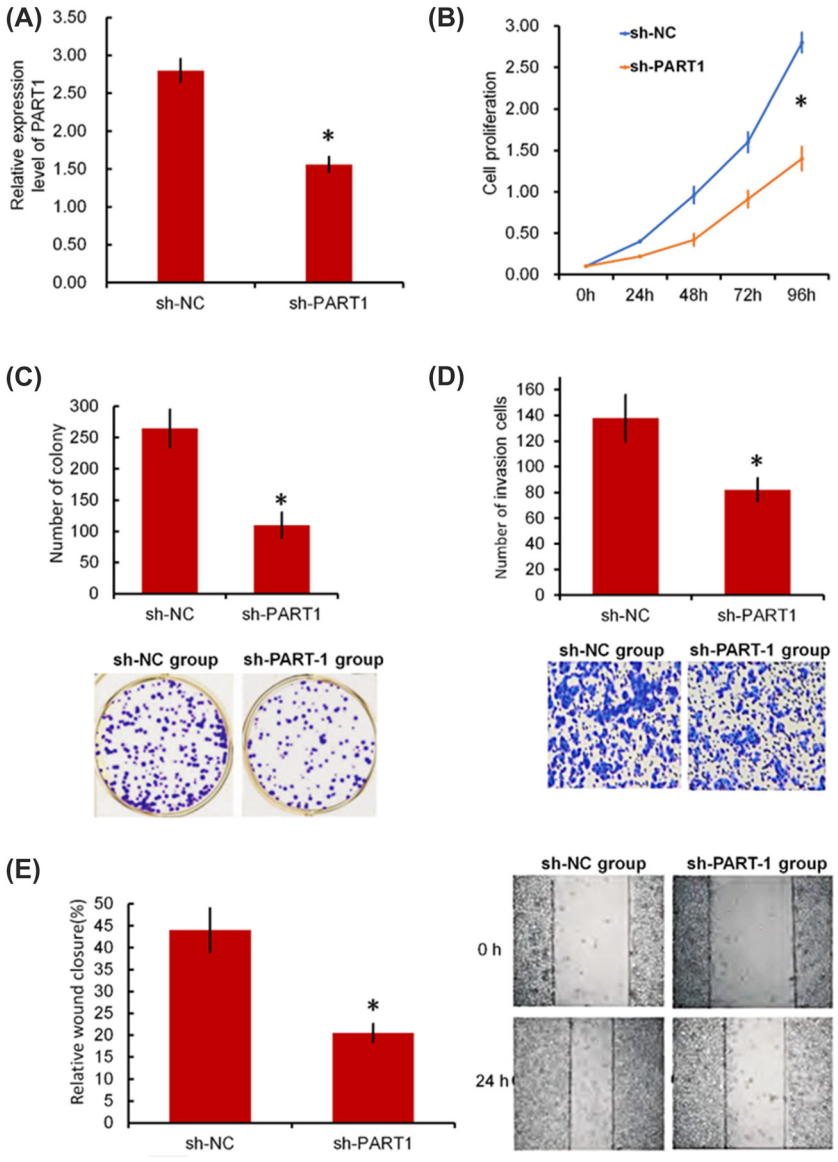

Figure 2: The effect of knocking down PART-1 on the proliferation, invasion, and migration of A549 cells. (A) The expression of PART-1 in A549 cells transfected with PART-1 shRNAs and negative control was validated by RT–qPCR. (B) The proliferation of sh-PART1 and sh-NC cells was determined by the CCK-8 assay. (C) Colony formation of sh-PART1 and sh-NC cells. (D, E) The cell invasion and wound healing results of sh-PART1 and sh-NC cells by Transwell invasion assay and wound healing assay. *$p<0.05$ sh-PART1 group vs. sh-NC group.

number of colonies formed by sh-PART1 cells and sh-NC cells was 110 and 265, respectively, as determined by colony formation assays (Figure 2C). sh-PART1 cells had significantly decreased numbers of colonies compared with sh-NC cells (Figure 2C, $p<0.05$). Cell invasion was detected by Transwell invasion assay. The average number of invaded cells was 82 and 138 for sh-PART1 cells and sh-NC cells, respectively, which means that cell invasion was inhibited by the downregulation of PART-1 (Figure 2D $p<0.05$). The migration of A549 cells was tested by wound healing assay. The results showed that migration was significantly reduced by downregulating PART-1 in sh-PART1 cells compared with sh-NC cells (Figure 2E).

Tumour development was inhibited by PART-1 downregulation in nude mice

An A549 tumour mouse model was generated to demonstrate the function of PART-1 in the development of tumours. The A549 cells of the sh-PART1 and sh-NC groups were inoculated into the axilla of nude mice, and the growth of the tumours was monitored. The size of the tumours was measured once every three days from 6 days after inoculation, and the results showed that the volume of the tumours increased over time (Figure 3A). The tumours were excised and weighed three weeks after injection, and the average tumour weight of the sh-PART1 group was 0.101 g, significantly lighter than that of the sh-NC group (0.221 g) (Figures 3B and C). The rate of tumour growth inhibition by the downregulation of PART-1 was 54.30%.

PART-1 targeted miR-204-3p and negatively regulated the expression of IGFBP-2

To investigate the molecular mechanism by which PART-1 modulates the growth of A549 cells, we predicted the targets of PART-1 using starBase v2.0 [22], and miR-204-3p was predicted as a possible target of PART-1. In addition, insulin-like growth factor binding protein 2 (IGFBP-2) was reported previously as a target of miR-204-3p [23]. We confirmed the binding between PART-1 and miR-204-3p and between IGFBP-2 and miR-204-3p. The WT or MT 3′-UTR of PART-1 containing the putative binding sites of miR-204-3p was inserted into the pmiR-GLO vector. Plasmids of WT or MT3′-UTR of PART-1 with miR-204-3p mimics were cotransfected, and a luciferase reporter assay was performed. The

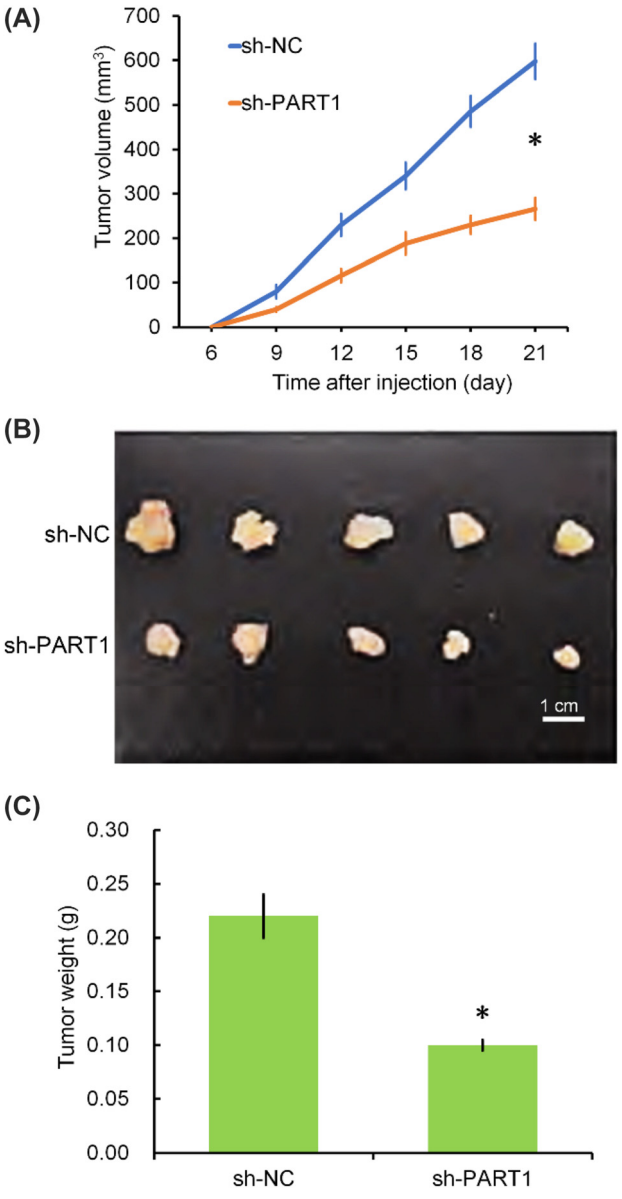

Figure 3: Downregulation of PART-1 reduced NSCLC tumour growth *in vivo*. Sh-PART1 and sh-NC cells were subcutaneously inoculated into nude mice (n=5 per group) at 1×107 per mouse. (A) Tumour volume from 6 to 21 days after inoculation. (B, C) Tumours excised from mice at 21 days after inoculation and average tumour weight. *$p<0.05$ sh-PART1 group vs. sh-NC group.

results showed that overexpression of the WT 3′-UTR of PART-1 significantly reduced the luciferase activity; however, the activity did not decrease when cells were transfected with the MUT 3′-UTR of PART-1 (Figure 4A). Meanwhile, the expression level of miR-204-3p increased significantly in the sh-PART1 cells compared with that in sh-NC cells by RT–qPCR

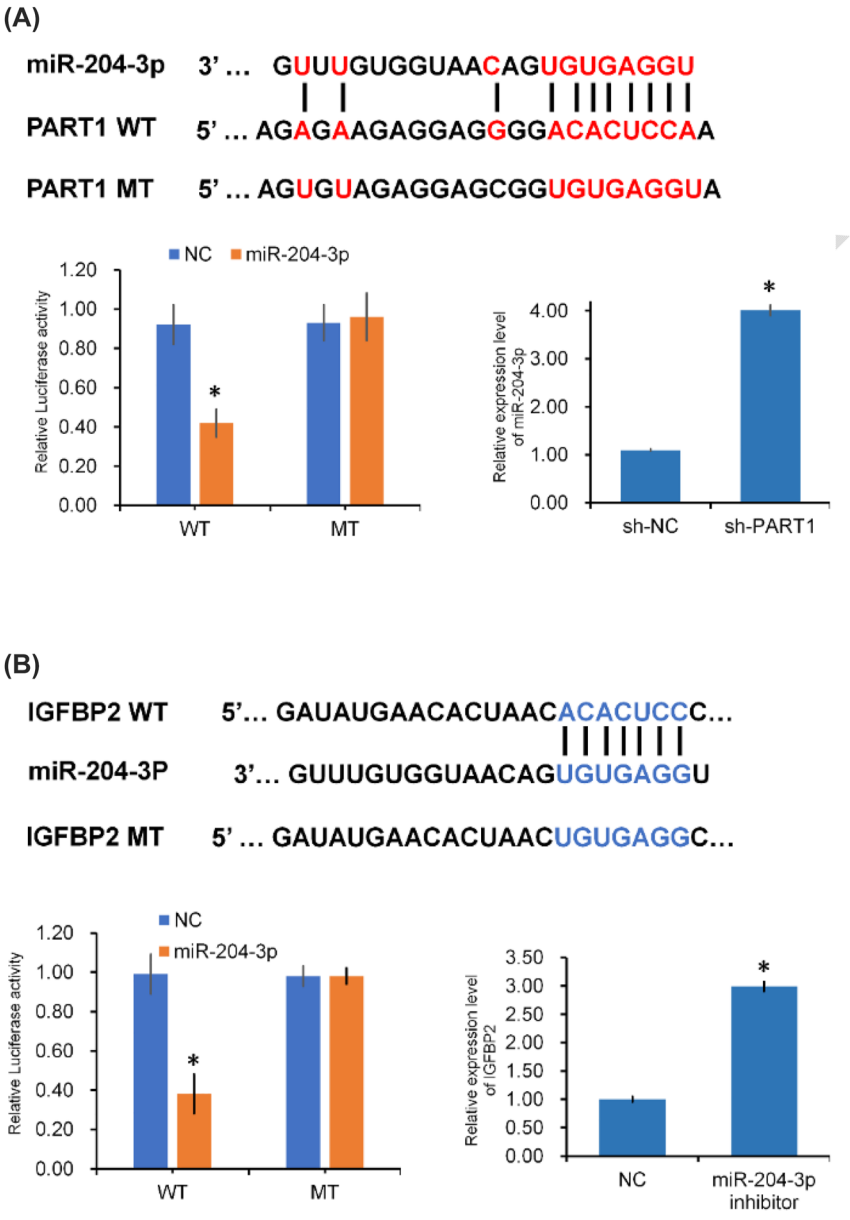

Figure 4: PART-1 targeted miR-204-3p and miR-204-3p targeted IGFBP-2. (A) The potential binding site between PART-1 and miR-204-3p; dual-luciferase reporter assays confirmed the interaction between PART-1 and miR-204-3p. The relative expression level of miR-204-3p in sh-PART1 cells compared with that in sh-NC cells. (B) The potential binding site between miR-204-3p and IGFBP-2 and dual-luciferase reporter assays indicated the interaction between miR-204-3p and IGFBP-2. The relative expression level of IGFBP-2 in miR-204-3p-inhibited cells compared with that in negative control cells. *Indicates $p<0.05$.

assay. These results indicated that the 3′-UTR of PART-1 bound miR-204-3p directly.

Overexpression of the WT 3′-UTR of IGFBP-2 significantly reduced the luciferase activity, but there was no remarkable decrease when overexpressing the MT 3′-UTR of IGFBP-2 (Figure 4B). Furthermore, the expression level was higher when miR-204-3p was inhibited in A549 cells (Figure 4B). The results indicated that miR-204-3p targeted the 3′-UTR IGFBP-2 directly.

Knocking down PART-1 inhibited the proliferation, invasion, and migration of A549 cells by regulating the miR-204-3p-targeted IGFBP-2 pathway

The expression level of IGFBP-2 mRNA or protein was markedly inhibited in PART-1-downregulated A549 cells, as detected using RT–qPCR assay or western blot, respectively ($p<0.05$, Figure 5). Meanwhile, the expression level was

partly rescued by transfecting the PART1-shRNA + miR204-3p inhibitor or PART1-shRNA + IGFBP2 overexpression vectors ($p<0.05$, Figure 5).

We performed serial experiments to investigate whether the knockdown of PART-1 affects the proliferation, invasion, and migration of A549 cells by the miR-204-3p-targeted IGFBP-2 pathway. The inhibition of proliferation, invasion, and migration was partly rescued in PART-1 knockdown A549 cells via downregulation of miR-204-3p or overexpression of IGFBP-2 ($p<0.05$, Figure 6).

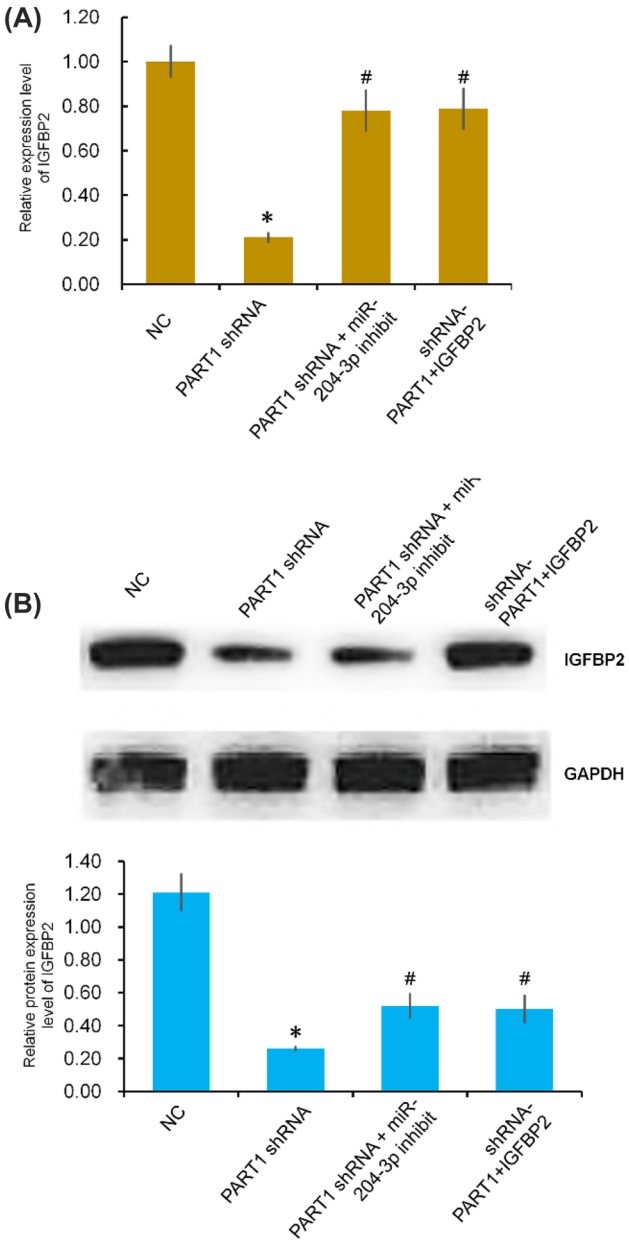

Figure 5: Effect of PART-1 and miR-204-3p on the expression of IGFBP-2 in the NC, PART1-shRNA, PART1-shRNA + miR204-3p inhibitor, and PART1-shRNA + IGFBP2 groups. (A) The relative expression level of IGFBP-2 mRNA was evaluated by quantitative RT–PCR. (B) The protein expression level of IGFBP-2 was evaluated by western blot. GAPDH was used as an internal control; *$p<0.05$, PART1-shRNA group compared with NC group; #$p<0.05$ compared with PART1-shRNA group.

Discussion

The vast majority (85%) of lung cancers are non-small cell lung cancer (NSCLC). Although this form of lung cancer progresses more slowly than SCLC, 40% of NSCLCs have spread beyond the lungs by the time they are diagnosed [3]. Elucidating the pathogenesis of NSCLC is valuable for controlling the disease [24]. LncRNAs promote cancer cell growth and development by sponging miRNAs [25].

In the last decade, lncRNAs have been proven to play crucial roles in lung cancer. Yu et al. identified and validated a list of 64 lncRNAs that were significantly dysregulated in NSCLC tumours with microarray gene expression analysis [14], but the functions of these lncRNAs remains to be elucidated *in vivo*. Nie et al. proved that lncRNA-UCA1 exerts oncogenic functions in NSCLC by targeting miR-193a-3p [15]; Liu et al. found that the lncRNA MALAT1 promoted lung cancer progression and inhibited cell apoptosis [26]. PART-1 (prostate androgen-regulated transcript 1) maps to chromosome 5q12, is predominantly expressed in the prostate and is regulated by androgens in human prostate cancer cells [16]. An increasing number of studies have shown that abnormally expressed PART-1 promotes the development of various tumours, such as breast cancer, cervical squamous cell carcinoma, and glioma [23, 27, 28]. Nonetheless, the impact of PART-1 on the development of NSCLC has remained unclear. Therefore, the current study aimed to elucidate the roles and mechanisms of PART-1 in NSCLC.

As expected, we found that the expression of PART-1 in NSCLC cells was higher than that in HBE cells. Next, we conducted a series of experiments to further elucidate the functional role of PART-1. The results showed that the downregulation of PART-1 inhibited the proliferation, invasion, and migration of A549 cells and that tumour growth was inhibited when PART-1 was knocked down in mouse tumour models. These results confirmed that PART-1 regulated NSCLC progression, which was consistent with a previous report on the function of PART-1 in several tumours, such as osteosarcoma, prostate cancer, and colorectal cancer [18, 19, 29].

LncRNAs play biological roles through various and distinct pathways in different systems [30, 31]. LncRNAs may serve as ceRNAs to promote tumour development. ceRNAs can sponge miRNAs, reducing their binding to target genes and thereby modulating their expression [7]. In the current

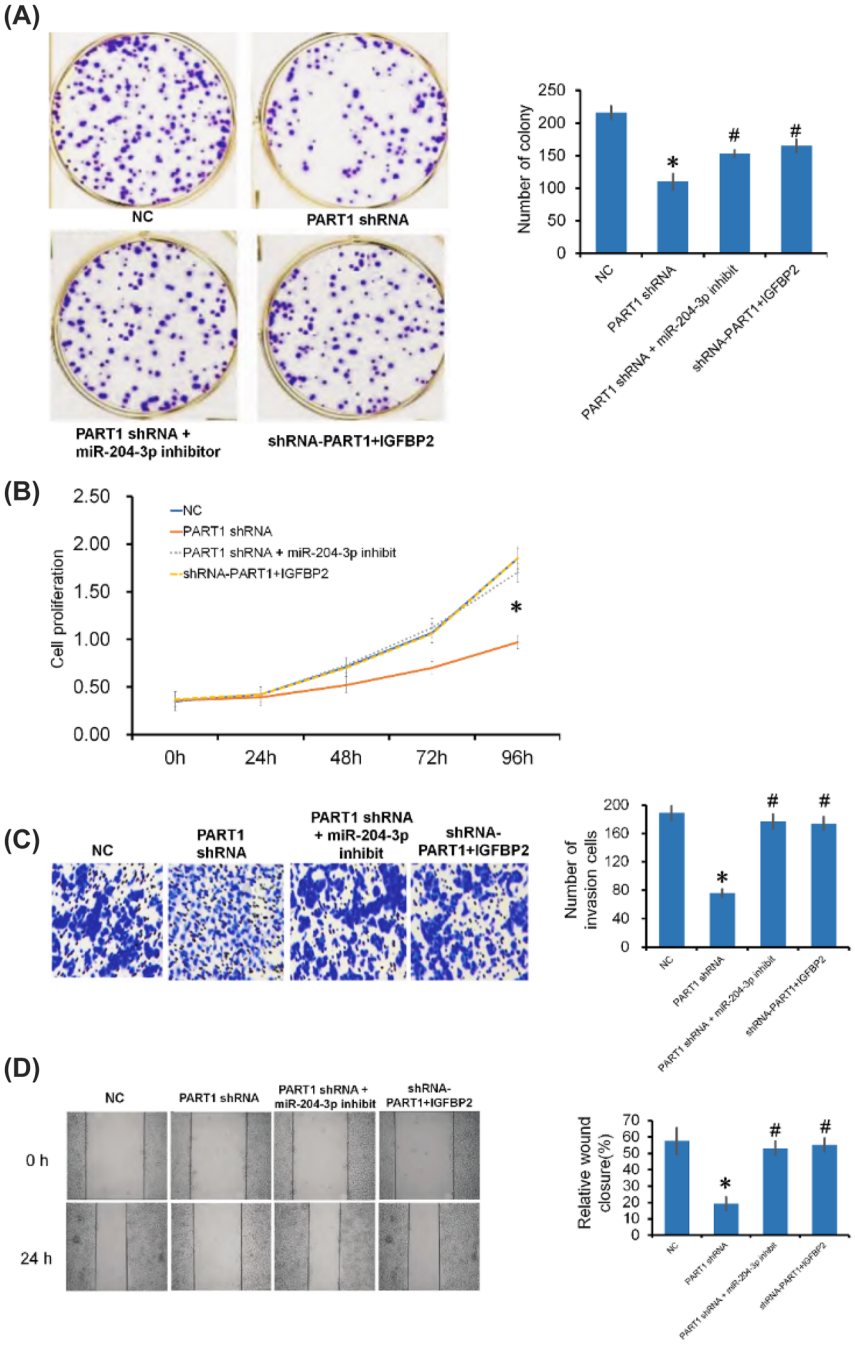

Figure 6: The downregulation of PART1 inhibited the proliferation, invasion, and migration of A549 cells by regulating the miR-204-3p-targeted IGFBP-2 pathway. (A) Colony formation of NC, PART1-shRNA, PART1-shRNA + miR204-3p inhibitor, and PART1-shRNA + IGFBP2 cells. (B) Cell proliferation, as determined by CCK-8 assay. (C, D) Cell invasion and wound healing assays of NC, PART1-shRNA, PART1-shRNA + miR204-3p inhibitor, and PART1-shRNA + IGFBP2 cells by Transwell invasion assay and wound healing assay. * *p<0.05, PART1-shRNA group compared with NC group; #p<0.05 compared with PART1-shRNA group.

study, we confirmed that PART-1 targeted miR-204-3p and that miR-204-3p targeted insulin-like growth factor binding protein 2 (IGFBP-2) directly. These results were consistent with previous findings, for example, that miR-204-3p targeted insulin-like growth factor binding protein 2 (IGFBP-2) directly and is involved in the development of glioma [23]. In addition, IGFBP-2 is involved in NSCLC progression, and the expression of IGFBP-2 in lung cancer patients was significantly higher than that in controls and increased with lung cancer progression to advanced stage [32]. Therefore,

PART-1 was proven to act as a promoter of NSCLC tumorigenesis by upregulating the miR204-3p/IGFBP-2 pathway by sponging miR-20b-5p.

Conclusions

Based on the combination of results produced in the current study, we conclude that PART-1 promotes the proliferation, invasion, and migration of NSCLC by regulating the miR204-3p/IGFBP-2 pathway. PART-1 might be a target for treating NSCLC; however, the relationship between the expression of PART-1 and the clinicopathological features and prognosis of NSCLC needs to be explored further. In addition, PART-1 might be an early marker in the diagnosis of early lung cancer.

Acknowledgments: The authors would like to express special thanks of gratitude to Dr. Sen Lian at Qingdao Agricultural University for his technical support to the study.
Research funding: This research received no external funding.
Author contributions: All authors have accepted responsibility for the entire content of this manuscript and approved its submission.
Competing interests: Authors state no conflict of interest.
Informed consent: Informed consent was obtained from all individuals included in this study.
Ethical approval: The study was conducted in accordance with the Decla-ration of Helsinki, and approved by the Institutional Animal Care and Use Committee (IACUC) of Chengyang People Hospital (IACUC:2017082600). Approval Date: 26 August 2017.

References

1. Gridelli C, Rossi A, Carbone DP, Guarize J, Karachaliou N, Mok T, et al. Non-small-cell lung cancer. Nat Rev Dis Prim 2015;1:15009.
2. Barta JA, Powell CA, Wisnivesky JP. Global epidemiology of lung cancer. Ann Glob Health 2019;85:8.
3. Bade BC, Cruz CSD. Lung cancer 2020: epidemiology, etiology, and prevention. Clin Chest Med 2020;41:1–24.
4. Xie S, Wu Z, Qi Y, Wu B, Zhu X. The metastasizing mechanisms of lung cancer: recent advances and therapeutic challenges. Biomed Pharmacother 2021;138:111450.
5. Schegoleva AA, Khozyainova AA, Fedorov AA, Gerashchenko TS, Rodionov EO, Topolnitsky EB, et al. Prognosis of different types of non-small cell lung cancer progression: current state and perspectives. Cell Physiol Biochem 2021;55:29–48.
6. Quinn JJ, Chang HY. Unique features of long non-coding RNA biogenesis and function. Nat Rev Genet 2016;17:47–62.
7. Statello L, Guo CJ, Chen LL, Huarte M. Gene regulation by long non-coding RNAs and its biological functions. Nat Rev Mol Cell Biol 2021;22: 96–118.
8. Hu Q, Ma H, Chen H, Zhang Z, Xue Q. LncRNA in tumorigenesis of non-small-cell lung cancer: from bench to bedside. Cell Death Dis 2022;8: 359.
9. Zhang Y, Xu Y, Feng L, Li F, Sun Z, Wu T, et al. Comprehensive characterization of lncRNA-mRNA related ceRNA network across 12 major cancers. Oncotarget 2016;7:64148–67.
10. He Q, Long J, Yin Y, Li Y, Lei X, Li Z, et al. Emerging roles of lncRNAs in the formation and progression of colorectal cancer. Front Oncol 2020;9: 1542.
11. Qiao Z, Dai H, Zhang Y, Li Q, Zhao M, Yue T. LncRNA NCK1-AS1 promotes cancer cell proliferation and increase cell stemness in urinary bladder cancer patients by downregulating miR-143. Cancer Manag Res 2020; 12:1661–8.
12. Qin CX, Yang XQ, Jin GC, Zhan ZY. LncRNA TSLNC8 inhibits proliferation of breast cancer cell through the miR-214-3p/FOXP2 axis. Eur Rev Med Pharmacol Sci 2019;23:8440–8.
13. Su P, Wang F, Qi B, Wang T, Zhang S. P53 regulation-association long non-coding RNA (LncRNA PRAL) inhibits cell proliferation by regulation of P53 in human lung cancer. Med Sci Mon Int Med J Exp Clin Res 2017; 23:1751–8.
14. Yu H, Xu Q, Liu F, Ye X, Wang J, Meng X. Identification and validation of long noncoding RNA biomarkers in human non-small-cell lung carcinomas. J Thorac Oncol 2015;10:645–54.
15. Nie W, Ge HJ, Yang XQ, Sun X, Huang H, Tao X, et al. LncRNA-UCA1 exerts oncogenic functions in non-small cell lung cancer by targeting miR-193a-3p. Cancer Lett 2016;371:99–106.
16. Lin B, White JT, Ferguson C, Bumgarner R, Friedman C, Trask B, et al. PART-1: a novel human prostate-specific, androgen-regulated gene that maps to chromosome 5q12. Cancer Res 2000;60:858–63.
17. Pu J, Tan C, Shao Z, Wu X, Zhang Y, Xu Z, et al. Long noncoding RNA PART1 promotes hepatocellular carcinoma progression via targeting miR-590-3p/HMGB2 axis. OncoTargets Ther 2020;13:9203–11.
18. Zhou T, Wu L, Ma N, Tang F, Zong Z, Chen S. LncRNA PART1 regulates colorectal cancer via targeting miR-150-5p/miR-520h/CTNNB1 and activating Wnt/β-catenin pathway. Int J Biochem Cell Biol 2020;118:105637.
19. Pan Z, Mo F, Liu H, Zeng J, Huang K, Huang S, et al. LncRNA prostate androgen-regulated transcript 1 (PART 1) functions as an oncogene in osteosarcoma via sponging miR-20b-5p to upregulate BAMBI. Ann Transl Med 2021;9:488.
20. Liu W, Li X, Tan X, Huang X, Tian B. MicroRNA-204-3p inhibits metastasis of pancreatic cancer via downregulating MGAT1. J BUON 2021;26: 2149–56.
21. Lee CC, Chen PH, Ho KH, Shih CM, Cheng CH, Lin CW, et al. The microRNA-302b-inhibited insulin-like growth factor-binding protein 2 signaling pathway induces glioma cell apoptosis by targeting nuclear factor IA. PLoS One 2017;12:e0173890.
22. Li JH, Liu S, Zhou H, Qu LH, Yang JH. starBase v2.0: decoding miRNA-ceRNA, miRNA-ncRNA and protein-RNA interaction networks from large-scale CLIP-Seq data. Nucleic Acids Res 2014;42:D92–7.
23. Chen PH, Chang CK, Shih CM, Cheng CH, Lin CW, Lee CC, et al. The miR-204-3p-targeted IGFBP2 pathway is involved in xanthohumol-induced glioma cell apoptotic death. Neuropharmacology 2016;110: 362–75.
24. Tang XJ, Wang W, Hann SS. Interactions among lncRNAs, miRNAs and mRNA in colorectal cancer. Biochimie 2019;163:58–72.

25. Seo D, Kim D, Chae Y, Kim W. The ceRNA network of lncRNA and miRNA in lung cancer. Genomics Inform 2020;18:e36.
26. Liu S, Jiang X, Li W, Cao D, Shen K, Yang J. Inhibition of the long non-coding RNA MALAT1 suppresses tumorigenicity and induces apoptosis in the human ovarian cancer SKOV3 cell line. Oncol Lett 2016;11: 3686–92.
27. Wang Z, Xu R. lncRNA PART1 promotes breast cancer cell progression by directly targeting miR-4516. Cancer Manag Res 2020;12:7753–60.
28. Liu H, Zhu C, Xu Z, Wang J, Qian L, Zhou Q, et al. lncRNA PART1 and MIR17HG as ΔNp63α direct targets regulate tumor progression of cervical squamous cell carcinoma. Cancer Sci 2020;111:4129–41.
29. Sun M, Geng D, Li S, Chen Z, Zhao W. LncRNA PART1 modulates toll-like receptor pathways to influence cell proliferation and apoptosis in prostate cancer cells. Biol Chem 2018;399:387–95.
30. Wu Y, Wang Y, Wei M, Han X, Xu T, Cui M. Advances in the study of exosomal lncRNAs in tumors and the selection of research methods. Biomed Pharmacother 2020;123:109716.
31. Chen M, Wu D, Tu S, Yang C, Chen D, Xu Y. A novel biosensor for the ultrasensitive detection of the lncRNA biomarker MALAT1 in non-small cell lung cancer. Sci Rep 2021;11:3666.
32. Tang D, Yao R, Zhao D, Zhou L, Wu Y, Yang Y, et al. Trichostatin A reverses the chemoresistance of lung cancer with high IGFBP2 expression through enhancing autophagy. Sci Rep 2018;8:3917.